Ultrathin films of Pd on Nb(111): Intermixing and effect of formation of a surface alloy

Jacek Brona and Antoni Ciszewski
Institute of Experimental Physics, University of Wroclaw, pl. M. Borna 9, PL 50-204 Wroclaw, Poland
(Received 19 October 2003; published 12 March 2004)

Pd/Nb(111) adsorption system was investigated by the LEED, AES, and CPD methods. Pd was deposited at room temperature, and annealed from 400 to 2150 K. The growth of Pd deposit follows the monolayer plus simultaneous multilayer growth mode. Up to 24 ML the deposit grows without a long-range order. For coverage higher than 24 ML, Pd(111) domains with the Pd$\langle 110\rangle$||Nb$\langle 211\rangle$ epitaxial relation appear. Similar domains are seen for coverage higher than 12 ML in the temperature range 400–900 K. Starting from 600 K the process of intermixing of Pd and Nb occurs for each annealed film thicker than 1 ML. It causes formation of the surface alloy with the (1×1) lateral periodicity with reference to Nb(111). The surface alloy exists from 800 K to 1400 K.

DOI: 10.1103/PhysRevB.69.115408 PACS number(s): 68.60.Dv, 61.14.Hg, 82.80.Pv

I. INTRODUCTION

There are numerous cases of the intermixing of components at the surface and subsurface regions for metal-on-metal adsorption systems.[1] This often leads to a bimetallic surface alloy formation. Surface alloys have attracted much attention recently, and investigations of them are a growing research field.[2,3] Understanding of the intermixing, segregation, and surface alloy formation phenomena is still not complete. Structural and compositional identification of changes of the Pd/Nb(111) adsorption system, occurring during deposition and annealing, helps to better understand these phenomena. There are many technological applications of bimetallic surfaces. They can exhibit physicochemical and catalytic properties that are very different from those of the surfaces of the individual metals. In particular, bimetallic systems containing Pd are very promising candidates for model and real catalysts.[4,5]

The main objective of this study was to investigate the intermixing process of adsorbate and substrate atoms and the possible effect of formation of a surface alloy. Until now, the Pd/Nb adsorption system was investigated for the (011) and (001) faces of Nb substrate. In both cases the intermixing of adsorbate and substrate atoms occurs from 600–700 K, for Pd films thicker than one monolayer (ML).[6–8] Pd atoms of adlayers thinner than 1 ML remain at the top of the surface. Intermixing of adsorbate and substrate atoms was also observed for other refractory bcc metals with a palladium adsorbate, such as Pd/Ta(011),[9,10] Pd/Mo(011),[11] Pd/Mo(001),[12,13] Pd/W(112),[14–16] and Pd/W(111).[17] These examples show that the intermixing of Pd and Nb atoms in the Pd/Nb(111) adsorption system is quite probable. Intermixing of Pd and Nb atoms in bulk crystals supports this supposition, too. Another phenomenon of importance, which is known for the systems Pd/W(111) and Pd/Mo(111), is faceting. W(111) and Mo(111) surfaces, coated with at least a single physical monolayer (three geometric monolayers) of palladium, undergo a massive reconstruction from a planar morphology to a microscopically faceted surface upon heating to $T>700$ K.[18–22] Three-sided nanometer-sized pyramids form, in which the sides are mainly Pd-covered {112} facets.[23] Low-energy electron diffraction is an appropriate tool to reveal such facets, therefore attention was also paid to search this phenomenon in our experiment.

II. EXPERIMENTAL

Low-energy electron diffraction (LEED), Auger electron spectroscopy (AES), and contact potential measurements (CPD) by Anderson's method implemented this investigation. The experiment was performed in an ultrahigh vacuum system with base pressure below 1×10^{-10} Torr, equipped with a four-grid spherical energy analyser with a retarding field used for LEED and AES, and an electromagnetically focused electron gun for CPD measurements. LEED patterns were videotape recorded. Intensity of LEED spots was calculated with a computer program after processing the analog video record into the digital one. Measurements were carried out on a single-crystal sample of Nb(111) cut within 0.15° accuracy. The sample was cleaned by heating at 1500 K in an oxygen atmosphere of 5×10^{-7} Torr in the first stage, which was followed by repeated flashing up to a temperature close to Nb melting point.[24] This procedure resulted in a surface for which no contaminants were detected by AES, and a good quality LEED pattern of the Nb(111) was obtained. The sample was heated by electron bombardment. The temperature of the sample was measured by a W–5%Re/W–26%Re thermocouple spot welded to the back side of the sample.

Pd was deposited by evaporation from resistively heated 0.2 mm diameter W wire wrapped with 0.1 mm diameter Pd wire of the purity 99.99%. The source was outgassed to deposit a clean Pd film at a rate of about 0.3 ML per min. We define 1 ML as a geometric monolayer with an atom density of 5.3×10^{14} atoms/cm^2. Calibration of Pd source is based on Auger uptake curves. The sample was kept at room temperature (RT) during deposition, and the pressure remained below 2×10^{-10} Torr. During annealing the sample was kept at a given temperature for 2.5 min, then heating was interrupted and the measurement was started after cooling the sample down to 340 K.

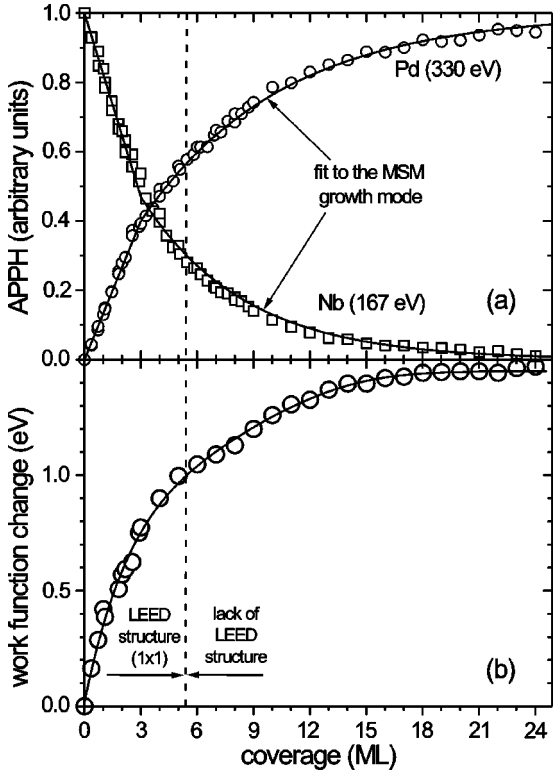

FIG. 1. Changes of (a) Auger peak-to-peak height and (b) work function as a function of Pd coverage.

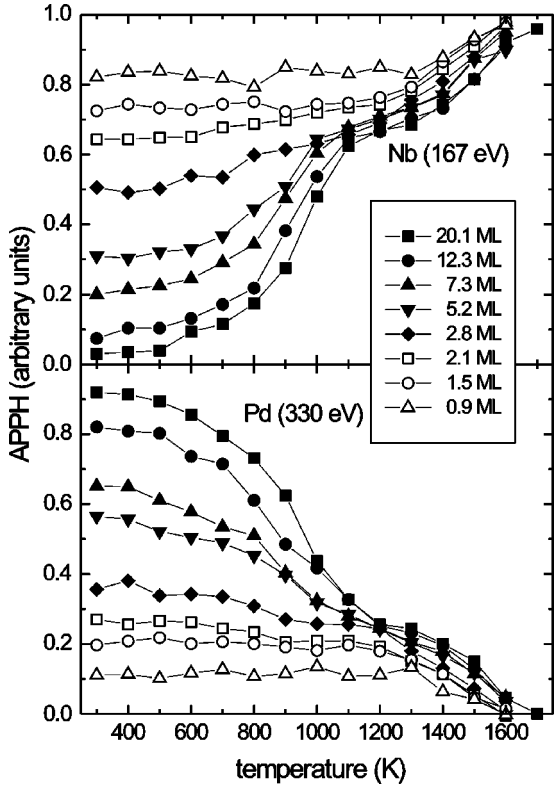

FIG. 2. Changes of Auger peak-to-peak height as a function of annealing temperature.

III. RESULTS

A. Deposition

The AES results obtained just after deposition from Auger peak-to-peak height (APPH) measurement of Nb (167 eV) and Pd (330 eV) as a function of Pd coverage are shown in Fig. 1(a). The Nb APPH is normalized to its bulk value, and the Pd APPH to the value of the thick film, where it saturates. Initially, Pd(Nb) APPH's are increasing (decreasing) linearly, until at 3 ML coverage they reach values of 0.40 and 0.47, respectively. Then the changes of APPH's are exponential. Work function (WF) changes as a function of Pd coverage are shown in Fig. 1(b). WF of clean Nb(111) surface is 4.36 eV.[25] Initial slope of the WF curve is steep and almost linear up to 3 ML. Then the WF is growing less intense and, beginning from about 20 ML, saturates to reach the value 1.45 eV above the clean Nb(111) surface work function. LEED pattern of the clean sample surface shows that the Nb(111) plane is unreconstructed. A good quality diffraction pattern is seen up to about 2 ML. In this coverage range the intensity of some spots is increasing, while that of the others is decreasing. Above 2 ML the intensity of all diffraction spots decreases with increasing coverage, and eventually all spots disappear at about 5.5 ML. Up to 24 ML there is no diffraction structure. A film thicker than 24 ML (about 30 ML) gives a faint pattern with broad spots of the fcc(111) plane of the lattice constant of palladium (3.89 Å). Epitaxial orientation with respect to the substrate is $\mathrm{Pd}\langle 110\rangle||\mathrm{Nb}\langle 211\rangle$.

B. Annealing

The AES data of annealing are presented in Fig. 2. For coverage 0.9 and 1.5 ML the AES signals from Nb and Pd are constant up to 1300 K and 1200 K, respectively. For 2.1 and 2.8 ML, there are four stages of AES variations. Up to 600–700 K the Nb (Pd) signals are constant, then they are increasing (decreasing) up to 900 K, then variations are relatively small, and finally above 1200–1300 K they go more intense towards the clean surface values. For films thicker than 3 ML there are four stages of AES variations as well, but they are better pronounced. Up to 700–800 K Nb (Pd)

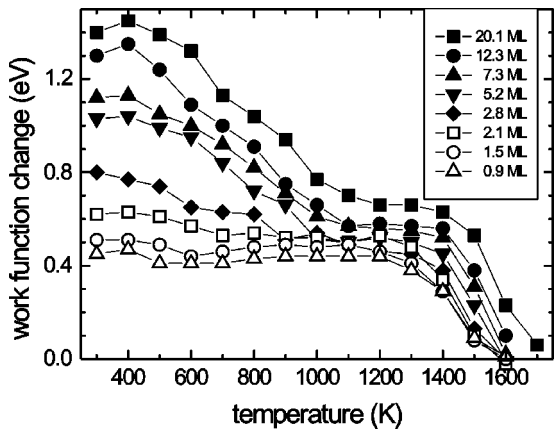

FIG. 3. Changes of work function as a function of annealing temperature.

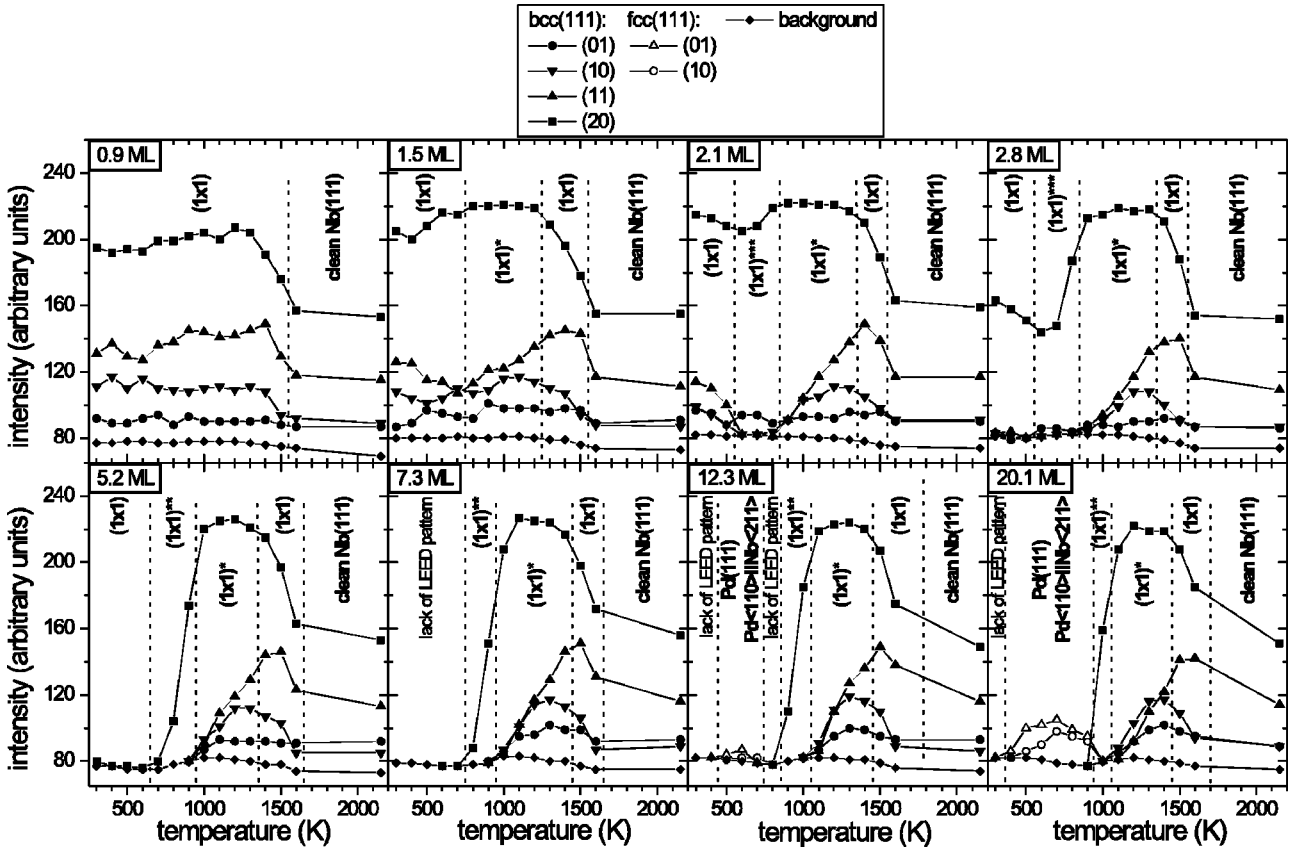

FIG. 4. Variations of the intensity of diffraction spots of Pd layers of various thickness as a function of annealing temperature.

signals increase (decrease) relatively slowly, then up to 1000–1100 K they change fast, then they increase (decrease) relatively slow again, and above 1300–1400 K they go more intense towards the clean surface values.

The CPD data of annealing are shown in Fig. 3. A notable feature for each coverage is a period of constant work function. Depending on coverage it occurs between 800 K and 1400 K. The higher the coverage the later the appearance of plateau and the later the disappearance. After disappearance of plateau the WF for each coverage goes to the value of clean Nb(111).

Variations of diffraction-spot intensity as a function of annealing temperature for coverage from 0.9 to 20.1 ML are shown in Fig. 4. The intensities were registered for the same value of the primary electron beam energy 108 eV and the same angle of incidence. During the plateau stage of WF the intensity of diffraction spots evolves in a similar way for every coverage higher than 1 ML. Such LEED patterns are marked (1×1)*. If only (20) spots are visible patterns are marked (1×1)**, and if only (20) and (01) spots are visible patterns are marked (1×1)***. A diagram, made in the temperature/coverage coordinate system, of all LEED patterns observed is shown in Fig. 5.

IV. DISCUSSION

A. Deposition

Variations of AES signals show that monolayer plus simultaneous multilayer (MSM) growth mode occurs. Breaks seen on the Auger uptake curves [Fig. 1(a)] indicate completion of the first monolayer. In this case, the first monolayer is a physical one, i.e., it consists of three geometric monolayers. Thickness of the first monolayer is given[26] by

$$d = -0.74\lambda_S \ln\left(\frac{I_S}{I_S^{\text{bulk}}}\right), \tag{1}$$

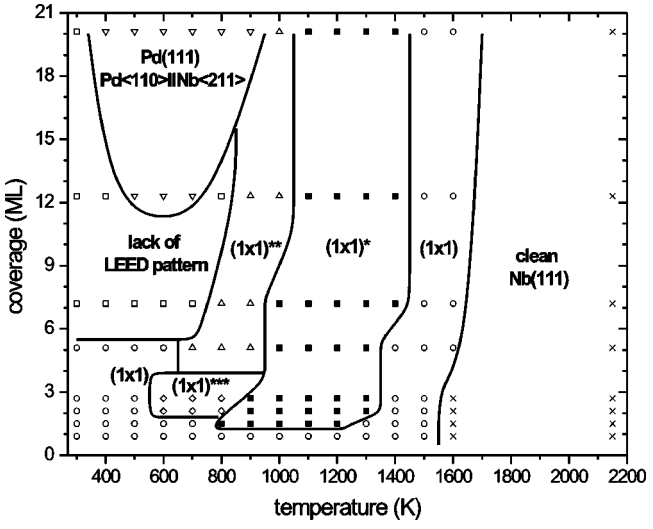

FIG. 5. Diagram of observed LEED patterns.

$$d = -0.74\lambda_A \ln\left(1 - \frac{I_A}{I_A^{\text{bulk}}}\right), \quad (2)$$

where d is the layer thickness, I_S is the substrate AES signal, I_A is the adsorbate signal, I_S^{bulk} is the clean substrate signal, I_A^{bulk} is the bulk adsorbate signal, λ_S is the inelastic mean free path (IMFP) of the electrons giving the substrate signal, and λ_A is the IMFP of the electrons giving the adsorbate signal. In this case I_S^{bulk} and I_A^{bulk} are equal to 1, $I_S = 0.47$ and $I_A = 0.40$. Thickness calculated from Eq. (1) is 3.1 Å for $\lambda_S = 5.5$ Å (a value calculated by Tanuma *et al.*[27]) or 3.0 Å for $\lambda_S = 5.4$ Å (a value estimated by Song *et al.*[18] for the Pd/W(111) system); considering the IMFP for Nb to be almost the same as that for W. Thickness of three monolayers calculated from Eq. (2) is 3.1 Å for $\lambda_A = 8.3$ Å (Ref. 27) or 2.6 Å for $\lambda_A = 6.8$ Å.[18] All these values are in good agreement with the triple spacing between the (111) planes of NB (2.86 Å). Variations of the signals for coverage higher than 1 ML are fit in accordance with the analysis proposed by Argile and Rhead[28] for the MSM growth mode. This is assumed that, for coverage higher than 1 ML, each adsorbate atom impinging on the surface sticks where it hits: there is no lateral motion. Nb uptake curve is fitted with the $\text{APPH}(\theta) = 0.47\{\exp[-0.53(\theta - 1)]\}$ function, and Pd uptake curve with the $\text{APPH}(\theta) = 0.60\{1 - \exp[-0.40(\theta - 1)]\} + 0.40$ function, where θ is coverage expressed in physical monolayers. Although calculated curves fit the experimental data very well, it should be realized that the higher the coverage the smaller the influence of impinging atoms on APPH. When APPH of Nb (Pd) is smaller (higher) than 0.05 (0.95) it is impossible to assess whether the MSM growth continues. This occurs for coverage higher than 16 or 22 ML for Nb and Pd signals, respectively. Therefore AES assessment of the growth mode in the Pd/Nb(111) system is reliable up to 22 ML.

The vanishing of diffraction pattern, which commences from 2 ML, indicates that the adlayer grows in the form of small clusters whose lateral extent is so small that it could not produce any diffraction pattern. Pd is not able to grow pseudomorphically on Nb(111) due to the difference in radius between Pd and Nb atoms (if we construct hard sphere models to reproduce the Pd fcc or the Nb bcc lattice, the diameter of the Pd spheres is 2.75 Å while that for Nb spheres is 2.86 Å). A faint diffraction pattern with broad spots of the fcc(111) plane with the lattice constant of Pd (3.89 Å) seen for 30 ML coverage shows that domains of Pd(111) appear on the surface. The orientation $\text{Pd}\langle 110\rangle || \text{Nb}\langle 211\rangle$ results from a relatively small misfit along these directions. Distance between neighbor atoms along the $\langle 211\rangle$ direction of Nb(111) is 8.08 Å, i.e., 98% of the distance between every third atom along the $\langle 211\rangle$ direction of Pd(111) (8.25 Å). Broad spots indicate that the lateral extent of these domains is smaller than the transfer width (about 100 Å) of the primary electron beam.[29] Although the lateral misfit is relatively small, transition from the bcc(111) that is a rough, rather loose packed plane to the smooth, close packed fcc(111) plane has to be highly strained. It is important to realize that the LEED method is more surface sensitive than AES. For this experiment, diffraction patterns originate from about 6 ML, while ''information depth'' (defined as the average distance normal to the surface from which 95% of the detected signal originates) estimated for AES measurements of Nb (Pd) is about 16 (22) ML. Therefore observation of Pd(111) domains for 30 ML coverage does not give direct information about the whole film, but only about few outermost ML.

B. Annealing

For 20.1 ML and 12.3 ML, LEED measurement shows the appearance of Pd(111) domains from 400 and 500 K, respectively. Pd atoms coalesce during annealing and form regions of the thickness sufficient to form the Pd(111) plane. For 20.1 ML, at RT the thickness of deposit is almost suitable to form Pd(111) domains, so at 400 K such domains are ready visible. For 12.3 ML, the deposit is thinner, so the process of coalescence has to last longer, and the Pd(111) structure is seen at 500 K. With increasing temperature the number of Pd(111) domains increases (intensifying LEED spots), reaching maximum at 600 K for 12.3 ML and at 700 K for 20.1 ML. Broad spots of LEED patterns indicate that the lateral extent of these domains is less than 100 Å. This is caused by a high strain in these domains. AES measurement shows that for 5.2 and 7.3 ML coalescence also occurs, but initial coverage is too low to form a Pd(111) plane.

Decreasing (increasing) of Pd (Nb) AES amplitude means that Pd atoms coalesce and/or the number of Pd atoms on the surface decreases. The amount of surface Pd atoms may decrease due to thermal desorption and/or intermixing of adsorbate and substrate atoms. Thermal desorption of Pd atoms is unlikely at temperature lower than 1000–1100 K. There is no data concerning Pd thermal desorption from Nb(111), but it should not differ from what was measured for W(111) and Mo(111). Pd atoms commence to desorb off W(111) at 1000–1100 K[18,30] and Mo(111) at 1050–1150 K.[20,21] As mentioned in introduction, intermixing is very probable, and indeed it occurs. Disappearance of Pd(111) domains shows that, for 12.3–20.1 ML, the process of intermixing occurs at least at 700–800 K. It results in the thinning of Pd adlayer, and therefore fcc domains cannot remain. Passing of the (1×1) LEED pattern into the (1×1)*** observed at 600 K for low coverage, which is accompanied by the decreasing (increasing) of Pd (Nb) Auger amplitudes, indicates that the intermixing commences from 600 K. At this temperature it is not an intensive process, therefore it does not affect thick Pd films. With increasing temperature the intermixing becomes significant, and eventually leads to formation of a surface alloy which is indicated by the LEED pattern (1×1)*. The alloy is characterized by a constant work function of $(4.9 \pm 0.1$ eV), and a high perfection of atomic structure evidenced by sharp and intense diffraction spots. The alloy is thermally stable. For 5.2–20.1 ML, AES clearly shows that after a period of relatively intense intermixing, during the alloy existence the number of Pd atoms on the surface decreases slowly. The variations of 2.1–2.8 ML AES measurement data are similar to those of thicker films, although less pronounced due to a lower initial coverage. The topmost

monoatomic layer of the alloy is composed of Pd atoms. Following observations support this supposition. First, atoms of an adlayer of the thickness 0.9 ML do not intermix with substrate atoms (no changes of LEED and AES are observed). This means that the remaining single monoatomic layer of Pd atoms on the top of the surface is preferred. Second, AES and LEED results obtained just after decay of the alloy are similar to those obtained for 1 ML on clean substrate. This suggests that the alloy decays as a result of decomposition of its subsurface structure, which results in the remaining Pd monolayer on the clean substrate. There is an open question what the structure of subsurface layers of the alloy could be. Preliminary field ion microscopy measurement conducted for the Pd/Nb adsorption system indicates that there is a substitutional solution of Pd atoms in Nb substrate.[31] Decay of the surface alloy is indicated by the lowering WF, increasing rate of the change of AES signals, and by the vanishing LEED pattern (1×1)*. It starts above 1200–1400 K, the higher the initial coverage the higher is the initial temperature of decay. The clean Nb(111) surface appears above 1500–1600 K, the higher the initial coverage is the later the clean surface appears.

In the Pd/W(111) and Pd/Mo(111) systems, arising {112} facets were observed. They were not noticed here. Probable reason for that is the intermixing of Pd and Nb atoms in the 700–1100 K range of temperature when faceting would be expected. In the Pd/W(111) and Pd/Mo(111) a physical monolayer of Pd ''floats'' on a faceted surface.[20,32,33] Perhaps such a behavior is a reflection of bulk properties. A substitutional solution of Pd in bulk crystal of W or Mo can contain up to 1.5% or 4% Pd atoms, respectively, while up to 20% in bulk crystal of Nb.[34]

V. SUMMARY

Growth of Pd deposit at room temperature follows the monolayer plus simultaneous multilayer growth mode (in this case simultaneous multilayers grow on a layer composed of three geometric monolayers). Up to 24 ML the Pd deposit grows without the long-range order. For coverage higher than 24 ML, Pd(111) domains with the Pd$\langle110\rangle||$Nb$\langle211\rangle$ epitaxial relation appear. Lateral extent of these domains is less than about 100 Å. Similar domains are seen for coverage higher than 12 ML in the temperature range 400–900 K. Starting from 600 K the process of intermixing of Pd and Nb occurs for every annealed film thicker than 1 ML. It causes formation of the surface alloy with the (1×1) lateral periodicity with reference to Nb(111). The WF of this state is found to be $(4.9\pm0.1$ eV) and the topmost monoatomic layer entirely consists of Pd atoms. The surface alloy exists from 800–1000 K to 1200–1400 K (the higher initial coverage the higher temperature). Atoms of adlayers thinner than 1 ML do not intermix with substrate atoms. No indication of faceting was found.

ACKNOWLEDGMENT

This work was supported by the University of Wroclaw, Grant No. 2016/W/IFD/00.

[1] *Growth and Properties of Ultrathin Epitaxial Layers*, edited by D. A. King and D. P. Woodruff (Elsevier, Amsterdam, 1998).
[2] U. Bardi, Rep. Prog. Phys. **57**, 939 (1994).
[3] *Surface Alloys and Alloy Surfaces*, edited by D.P. Woodruff, (Elsevier, Amsterdam, 2002).
[4] J.A. Rodriguez, Surf. Sci. Rep. **24**, 223 (1996).
[5] J. C. Bertolini and Y. Jugnet, in *Surface Alloys and Alloy Surfaces*, edited by D.P. Woodruff (Elsevier, Amsterdam, 2002), p. 404; J. A. Rodriguez, *ibid.* p. 438.
[6] M. Sagurton, M. Strongin, F. Jona, and J. Colbert, Phys. Rev. B **28**, 4075 (1983).
[7] A. Ciszewski, J. Brona, S. M. Zuber, Z. Szczudlo, and Ya. Losovyi, Prog. Surf. Sci. (to be published).
[8] J. Brona and A. Ciszewski, Appl. Surf. Sci. (to be published).
[9] M.W. Ruckman, V. Murgaiand, and M. Strongin, Phys. Rev. B **34**, 6759 (1986).
[10] B.E. Koel, R.J. Smith, and P.J. Berlowitz, Surf. Sci. **231**, 325 (1990).
[11] Ch. Park, E. Bauer, and H. Poppa, Surf. Sci. **154**, 371 (1985).
[12] D. Wu, W.K. Lau, Z.Q. He, Y.J. Feng, M.S. Altman, and C.T. Chan, Phys. Rev. B **62**, 8366 (2000).
[13] J. Heitzinger, S.C. Gebhard, D.H. Parker, and B.E. Koel, Surf. Sci. **260**, 151 (1992).
[14] J.J. Kolodziej, K. Pelhos, I.M. Abdelrehim, J.W. Keister, J.E. Rowe, and T.E. Madey, Prog. Surf. Sci. **59**, 117 (1998).
[15] J.J. Kolodziej, T.E. Madey, J.W. Keister, and J.E. Rowe, Phys. Rev. B **62**, 5150 (2000).
[16] K. Pelhos, I.M. Abdelrehim, C.-H. Nien, and T.E. Madey, J. Phys. Chem. B **105**, 3708 (2001).
[17] J.J. Kolodziej, T.E. Madey, J.W. Keister, and J.E. Rowe, Phys. Rev. B **65**, 075413 (2002).
[18] K.-J. Song, C.-Z. Dong, and T.E. Madey, Langmuir **7**, 3019 (1991).
[19] C.-Z. Dong, J. Guan, R. A. Campbell, and T. E. Madey in *The Structure of Surfaces IV*, edited by X. Xie, S. Y. Tong, and M. A. van Hove (World Scientific, Singapore, 1994), p. 328.
[20] K.-J. Song, J.C. Lin, M.Y. Lai, and Y.L. Wang, Surf. Sci. **327**, 17 (1995).
[21] J. Guan, R.A. Campbell, and T.E. Madey, J. Vac. Sci. Technol. A **13**, 1484 (1995).
[22] T.E. Madey, C.-H. Nien, K. Pelhos, J.J. Kolodziej, I.M. Abdelrehim, and H.-S. Tao, Surf. Sci. **438**, 191 (1999).
[23] C.-H. Nien and T.E. Madey, Surf. Sci. **380**, L527 (1997).
[24] R. Franchy, T.U. Bartke, and P. Gassmann, Surf. Sci. **366**, 60 (1996).
[25] H.B. Michaelson, J. Appl. Phys. **48**, 4729 (1977).
[26] M.P. Seah, Surf. Sci. **32**, 703 (1972).
[27] S. Tanuma, C.J. Powell, and D.R. Penn, Surf. Interface Anal. **11**, 577 (1988).
[28] C. Argile and G.E. Rhead, Surf. Sci. Rep. **10**, 277 (1989).
[29] G. Ertl and J. Kuppers, *Low Energy Electrons and Surface Chemistry* (VCH, Veinheim, 1985), p. 233.

[30] J. Kolaczkiewicz and E. Bauer, Surf. Sci. **420**, 157 (1999).
[31] J. Brona (unpublished).
[32] C. Dong, L. Zhang, U. Diebold, and T.E. Madey, Surf. Sci. **322**, 221 (1995).
[33] T.E. Madey, C.-H. Nien, K. Pelhos, J.J. Kolodziej, I.M. Abdelrehim, and H.-S. Tao, Surf. Sci. **438**, 191 (1999).
[34] *Binary Alloy Phase Diagrams*, edited by T. B. Massalski (ASM International, 1992).